17th Canadian Hydrotechnical Conference
17ième congrès spécialisé hydrotechnique canadienne

Hydrotechnical Engineering: Cornerstone Of A Sustainable Environment
Edmonton, Alberta, August 17–19, 2005 / 17–19 Août 2005

RIVER2D MORPHOLOGY, PART II: CURVED ALLUVIAL CHANNELS

J.A. Vasquez[1], P.M. Steffler[2] and R.G. Millar[1]
1. Department of Civil Engineering, The University of British Columbia, Vancouver, BC, Canada
2. Department of Civil and Environmental Engineering, The University of Alberta, Edmonton, AB, Canada

ABSTRACT: The model River2D-MORphology presented in the companion paper (Part I) was extended to simulate flow in curved alluvial channels by including two additional sub-models. These sub-models take into account the effects of the secondary flow on the direction of the bed shear stress and the influence of the lateral bed slope on the direction of bedload sediment transport. The model was tested using data from three experiments conducted in two flumes: (1) A weakly curved 140° channel and (2) a strongly curved 180° channel. The numerical model was able to reproduce the bed equilibrium profiles; including the "overshooting" of the bed profile downstream of the bend entrance that causes a point bar in the inner bank and deep pool in the outer bank. The model results showed better agreement with the weakly curved channel; for the strongly curved channel the model did not accurately reproduce the bed profile around the middle of the bend. This result can be explained because depth-averaged models neglect the transfer of flow momentum between the primary and secondary flows; which increases with flow curvature. However, given that most natural rivers have low curvatures, River2D-MOR should provide satisfactory results for real meandering rivers.

1. INTRODUCTION

Bends are very common features of natural rivers and their importance in river engineering practices is well recognized. Flow of water and sediment in erodible bends is extremely complex for the presence of a three-dimensional (3D) spiral motion, which generates erosion in the outer bank and deposition of sediment in the inner bank. Erosion can destroy or undermine structures located in the river; while deposition (point bars) may block water intakes or navigation canals. Thus, prediction of erosion and deposition patterns in erodible rivers is a very important and challenging task for river engineers, who usually resort to 2D numerical models for that purpose.

The bedload sediment transport model, River2D-MORphology, introduced in a companion paper (Vasquez et al. 2005) was extended to deal with flow in bends by adding two additional sub-models. These sub-models take into account the effects of the secondary flow on the direction of the bed shear stress and the influence of the lateral bed slope on the direction of bedload sediment transport, as discussed below.

1.1. Bedload sediment model

By considering only bedload transport and neglecting grain sorting, the 2D sediment continuity equation may be written as (Struiksma et al. 1985, Struiksma 1989, Kassem and Chaudhry 2002)

[1] $$(1-\lambda)\frac{\partial z_b}{\partial t}+\frac{\partial q_{sx}}{\partial x}+\frac{\partial q_{sy}}{\partial y}=0$$

q_{sx} and q_{sy} are the components in the x and y directions (horizontal plane) of the volumetric rate of bed-load transport per unit length q_s, λ is the porosity of the bed material (a default value of 0.4 is assumed), t is time and z_b the bed elevation. The components of the sediment transport rate depend on the sediment transport direction α and the bed slopes in the x and y directions $\partial z_b/\partial x$ and $\partial z_b/\partial y$

[2a] $$q_{sx}=q_s\left(1-\varepsilon K_s\frac{\partial z_b}{\partial x}\right)\cos\alpha$$

[2b] $$q_{sy}=q_s\left(1-\varepsilon K_s\frac{\partial z_b}{\partial y}\right)\sin\alpha$$

K_s is a calibration coefficient. ε is the sign of the bed slope relative to the flow direction: $\varepsilon = 1$ if the flow is going up-slope or $\varepsilon = -1$ if it is going down-slope.

The sediment transport rate q_s can be computed from many of the equations available. In this study the The Engelund-Hansen sediment transport equation was adopted (Kassem and Chaudhry 2002)

[3] $$q_s=0.05\frac{C^2}{g}\sqrt{g(G_s-1)D_{50}^3}\,(\tau^*)^{5/2}$$

C is the Chézy roughness coefficient, G_s is the specific gravity of the sediment, D_{50} the median grain diameter, g is the gravitational acceleration and τ^* is the dimensionless shear stress (Shield's parameter).

[4] $$\tau^*=\frac{u^2+v^2}{C^2(G_s-1)D_{50}}$$

u and v are the depth-averaged components of the velocity vector in the x and y directions respectively.

1.2. Influence of transversal bed slope

When the bed is flat, the direction α of bedload transport coincides with the direction δ of the bed shear stress. However, in sloping beds the gravity force induces a deviation between α and δ which can be taken into account by (Koch and Folkstra 1981, Struiksma et al. 1985, Talmon et al. 1995)

[5] $$\tan\alpha=\frac{\sin\delta-\frac{1}{f_s\tau^*}\frac{\partial z_b}{\partial y}}{\cos\delta-\frac{1}{f_s\tau^*}\frac{\partial z_b}{\partial x}}$$

f_s is a shape factor that ranges between 1 and 2 (Struiksma et al. 1985). In alluvial bends, equation 5 is necessary because a transversal bed slope develops between the outer and inner banks of the bend, caused by scour and deposition. In general, the transversal slope (and hence scour and deposition) increases with increasing values of f_s.

1.3. Influence of secondary flow (helical motion)

The difference between flow in a straight and a curved channel is the presence of centrifugal acceleration in the latter (or centripetal depending on the reference frame). Assuming a simple 1D streamline, the

centrifugal acceleration is $a_c = u^2/r_c$, where r_c is the radius of curvature of the streamline. Since the flow velocity distribution in the vertical is zero at the bottom and maximum close to the water surface, a_c reaches a maximum value close the water surface. Therefore, in a transversal cross section to the bend the surface layers of water are pushed in the outward direction. To fulfill mass continuity (zero mass flux in the transversal direction), water in the lower layers (close to the bed) move in the inward direction. When this secondary flow circulation combines with the primary flow motion in the longitudinal direction, it generates a complex 3D helical or spiral motion, characteristic of flow in bends. The inward motion near the bed transports sediment from the outer bank, where scour occurs, towards the inner bank, where deposition occurs. Therefore, the magnitude of the bed changes in a bend is linked to the intensity of the secondary motion.

A simple indicator of the intensity of the secondary motion can be obtained by using the Chezy friction equation $u = C(hS)^{1/2}$

[6] $$\frac{a_c}{g} = \left(\frac{C}{\sqrt{g}}\right)^2 \left(\frac{h}{r_c}\right) S$$

Being S the energy slope and h the water depth. In a 2D case, the distribution of horizontal velocity is also important for the intensity of the secondary flow (Blanckaert and Graf 2004).

The secondary flow causes the direction δ of the bed shear stress to deviate from the direction arctan(v/u) of the mean depth-averaged flow velocity (streamlines). This 3D effect cannot be simulated by a 2D depth-averaged model. Therefore semi-empirical secondary flow corrections must be introduced assuming a locally fully developed curved spiral flow (Rozovskii 1957, Struiksma et al. 1985)

[7] $$\delta = \arctan\left(\frac{v}{u}\right) - \arctan\left(A\frac{h}{r_c}\right)$$

The term $\delta_s = -\arctan(Ah/r_c)$ is the deviation of the bed shear stress relative to the streamlines, caused by the secondary flow. The parameter A is a function of Von Karman constant κ and Chezy's roughness coefficient.

[8] $$A = \frac{2}{\kappa^2}\left(1 - \frac{\sqrt{g}}{\kappa C}\right)$$

Equations 6 and 7 suggest that the flow curvature h/r_c is the main parameter for the scour and deposition in bends. Higher values of h/r_c will tend to increase both the scour and deposition along the bend. Unfortunately, equation 7 is strictly applicable to weakly curved bends only; for strongly curved bends, it tends to overestimate the effects of the secondary motion (Blanckaert and Graf 2004).

1.4. Curvature and inertial adaptation

The local radius of curvature of the streamlines is defined as

[9] $$r_c = \frac{|\vec{u}|^3}{|\vec{u} \times \vec{a}_c|}$$

Assuming steady state ($\partial u/\partial t = 0$, $\partial v/\partial t = 0$), equation 9 can be approximated as

[10] $$r_c = \frac{(u^2 + v^2)^{3/2}}{-uv\frac{\partial u}{\partial x} - v^2\frac{\partial u}{\partial y} + u^2\frac{\partial v}{\partial x} + uv\frac{\partial v}{\partial y}}$$

Equation 10 has the advantage of being applicable to channels of varying curvature, i.e. it is not limited to bends of constant radius of curvature (circular bends). Starting from a flat bed, the curvature will slowly adapt to the final bed topography. Equation 10 can be applied at every time step during the simulation to dynamically compute the curvature; however, that process is time consuming and might lead to numerical instabilities if the velocity gradients vary suddenly. An alternative approach is to apply equation 10 only at the beginning of the simulation to compute the initial curvature. Since that initial curvature lags behind the final value, an inertial adaptation equation is required (Rozovskii 1957, Struiksma et al. 1985)

[11] $$\beta\frac{C}{\sqrt{g}}\frac{h}{\sqrt{u^2+v^2}}\left(u\frac{\partial}{\partial x}\left(\frac{1}{r_c}\right) + v\frac{\partial}{\partial y}\left(\frac{1}{r_c}\right)\right) + \frac{1}{r_c} = \frac{\left|\vec{u}\times\vec{a}_c\right|}{\left|\vec{u}\right|^3}$$

The calibration parameter β varies normally between 0.4 and 2.0. Equation 11 reduces to equation 9 if the spatial gradients of curvature vanish. Therefore, equation 11 affects mostly the areas where curvature changes, such as the entrance and exit of a bend, its main effect is to shift the computed profiles towards the downstream direction.

Although the radius of curvature remains constant during the simulation, depth and velocity do not; thus, the bed shear stress direction δ changes dynamically according to equation 7.

1.5. Objectives

The main objective of this study is to assess the capabilities of River2D-MORphology to simulate the bed elevation changes in alluvial curved channels. Three laboratory experiments have been selected for comparison; two of them have a weak curvature, while the other has a strong curvature. As expected, the computed bed profiles agreed better with the measurements of the weakly curved channels.

2. EXPERIMENTAL DATA AND NUMERICAL MODEL

We selected three experiments of bed deformation in alluvial channels (Struiksma et al. 1985) to assess the numerical model. These experiments were performed in weakly and strongly curved alluvial channels composed of uniform sand with a specific gravity G_s = 2.65. The main characteristics of the experiments are summarized on Table 1. Two of experiments, called T1 and T2, were performed at the Delft Hydraulics Laboratory (DHL) 140° curved flume, which is a relatively long (L_c/B = 29.32) and weakly curved channel (h/R_c = 1/150 ~ 1/120), as shown on Fig. 1. The other experiment, T6, was performed at the Laboratory of Fluid Mechanics (LFM) 180° curved flume, which is a channel with a relatively shorter (L_c/B = 7.85) and narrower bend (B/h = 8.5) with a much stronger curvature (h/R_c = 1/21), as shown on Fig. 1. These experiments were selected because they provide the opportunity to assess the influence of channel curvature on the performance of the numerical model.

Several researchers (e.g., Koch and Flokstra 1981, De Vriend and Struiksma 1983, Struiksma et al. 1985, Struiksma 1989, Johannesson and Parker 1989 and Kassem and Chaudhry 2002) have used some of these experiments for their analytical or numerical models. Most of those models are based on curvilinear coordinates and structured grids. In contrast, River2D uses unstructured meshes made of triangular elements in a Cartesian coordinate system. The meshes of both flumes had the computational nodes spaced roughly 0.20 m apart. The DHL flume mesh was made of 6051 elements connected in 3456 nodes; while the LFM flume mesh was made of 3831 elements with 2150 nodes.

The boundary conditions for the hydrodynamic model were constant discharge in the upstream inflow section, and constant water surface elevation in the downstream outflow section. To avoid sediment flux

across the sidewalls, the direction of sediment transport was set equal to the direction of the mean flow at the lateral sidewalls: $\tan\alpha$ = v/u. The bed elevation of both the inflow and outflow sections was kept constant ($\partial z_b/\partial t = 0$).

To minimize the influence of boundary conditions, we artificially increased the length of the straight reaches upstream and downstream of the bends in the numerical model. The adopted lengths were 15 m for the DHL flume and 10 m for the LFM flume (Fig. 1).

Table 1. Main parameters of the experiments in alluvial bends performed at the Delft Hydraulics Lab (DHL), the Laboratory of Fluid Mechanics (LFM) curved channels (Struiksma et al. 1985).

Parameter	Symbol	DHL Flume T1	DHL Flume T2	LFM Flume T6
Discharge	Q (m^3/s)	0.047	0.061	0.170
Flume width	B (m)	1.5	1.5	1.7
Water depth	h (m)	0.08	0.10	0.20
Flow velocity	U (m/s)	0.39	0.41	0.50
Water slope	S (%)	0.236	0.203	0.180
Chézy coefficient	C ($m^{1/2}/s$)	28.4	28.8	26.4
Median grain diameter	D_{50} (mm)	0.45	0.45	0.78
Sediment transport	q_s (m^2/s)	7.2×10^{-6}	6.9×10^{-6}	13×10^{-6}
Shield's parameter	τ^* (-)	0.26	0.27	0.28
Bend radius	R_c (m)	12	12	4.25
Bend length	L_c (m)	29.32	29.32	13.35
Relative bend length	L_c / B (-)	19.55	19.55	7.85
Width-depth ratio	B / h (-)	18.75	15.00	8.50
Depth-radius ratio	h / R_c (-)	1/150	1/120	1/21
Secondary flow intensity	a_c / g (-)	0.0013	0.0014	0.0060

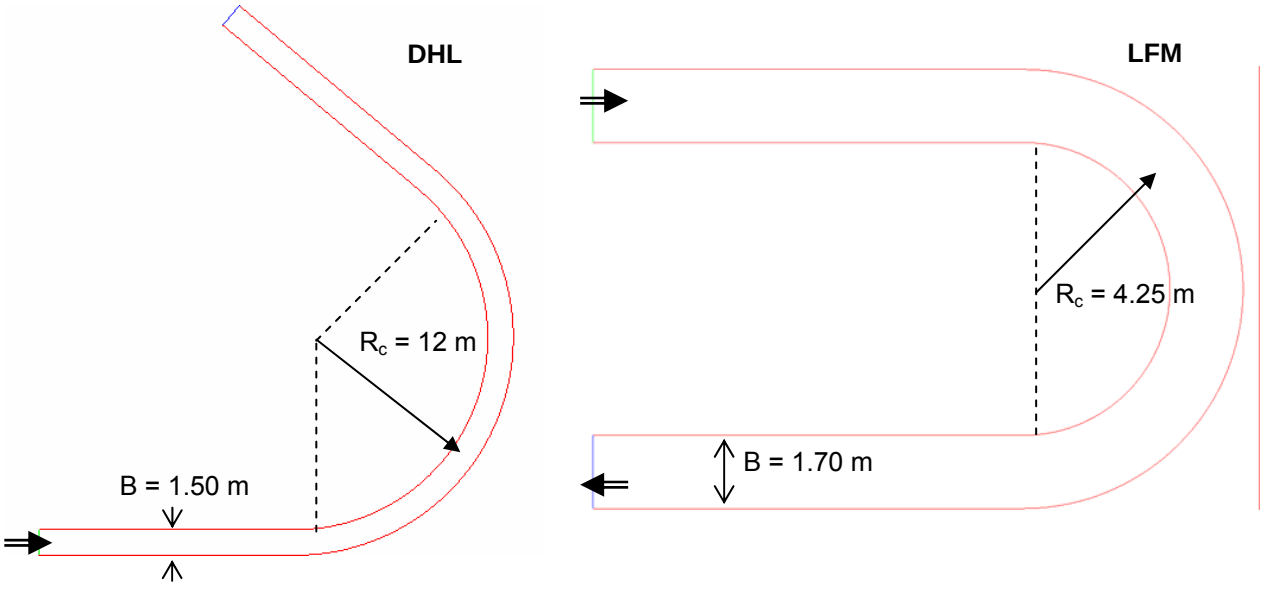

Figure 1. Delft Hydraulics Lab (DHL) 140° curved flume and Laboratory of Fluid Mechanics (LFM) 180° curved flume. Straight reaches up/downstream of bends are 15 m for DHL flume and 10 m for LFM flume.

3. RESULTS

Following the experimental conditions, all the simulations started from an initial flat bed and continued until bed equilibrium was reached (i.e. negligible bed changes observed, $\partial z_b/\partial t \approx 0$). A constant shape factor value of $f_s = 2.0$ was used for the three experiments. However, the values of the inertial adaptation parameter were different for the three experiments: $\beta = 2.0$ for T1, $\beta = 1.0$ for T2 and $\beta = 0.4$ for T6.

The influence of the calibration coefficient K_s in equation 2 did not seem to have a strong influence in the computed bed changes. For the experiments T1 and T2 it was set to zero $K_s = 0$, while for experiment T6 the small value $K_s = 0.2$ was adopted. The effect of $K_s = 0.2$ in experiment T6 was to slightly increase the magnitude of the maximum scour depth to better match the measured data.

Figure 2 shows the comparison between the measured and computed equilibrium bed profiles for DHL flume, experiments T1 and T2. Similar results for flume LFM, experiment T6, are shown in Figure 3. The longitudinal bed profiles shown are located some distance away from the right and left banks: 0.375 m (0.25B) for the DHL flume and 0.34 m (0.20B) for the LFM flume.

The relative depth in the ordinate of Fig. 2 and Fig. 3 represents the equilibrium water depth relative to the initial depth. Values of relative depth larger than 1 represent scour, while values smaller than 1 represent deposition. Along the bend, scour is observed in the outer (concave) bank and deposition in the inner (convex) bank. However, that pattern switches in the straight reach downstream from the bend, where decaying alternate bars develop. The numerical model was able to successfully reproduce that alternate bar pattern.

The best overall results were obtained for experiment T2. The agreement between the measured and computed profiles is very good, the magnitude and location of the bed oscillations is well reproduced. This experiment was also more numerically stable, we could apply a large time step of $\Delta t = 120$ s. At the beginning of the simulation the maximum bed shear deviation angle was $\delta_s = 5^o$, proving that curvature effects were not very intense.

During the numerical simulation of experiment T1, a bar was observed migrating from downstream of the first point bar and towards the bend exit. This migrating bar finally ended merging with the bar located at the bend exit. For T1, we used a smaller time step $\Delta t = 100$ s to prevent instabilities. At the beginning of the simulation the maximum bed shear deviation angle was $\delta_s = 4^o$

Experiment T6 was simulated using a time step $\Delta t = 60$ s. The initial bed shear stress deviation angle reached a maximum value of $\delta_s = 37^o$. This high value of δ_s indicates that the effects of the secondary flow are very strong in this case, as expected from the corresponding high values of the flow curvature. It is also observed in Fig. 3 that some degradation is predicted downstream of the bend, that has not been observed in the experiments.

The time step Δt was selected such that the maximum bed change Δz_b in any given time step is smaller than 5% of the original water depth. That usually prevents the model from becoming unstable as a consequence of large changes in the bed elevation during the computations.

4. DISCUSSION

River2D-MOR seems to reproduce the mean features of the bed elevation changes along the three alluvial bends simulated. Notably, the overshooting of the bed profile downstream of the bend entrance, where maximum scour and deposition occur (Struiksma et al. 1985, Parker and Johannesson 1989, Struiksma 1989) is correctly predicted.

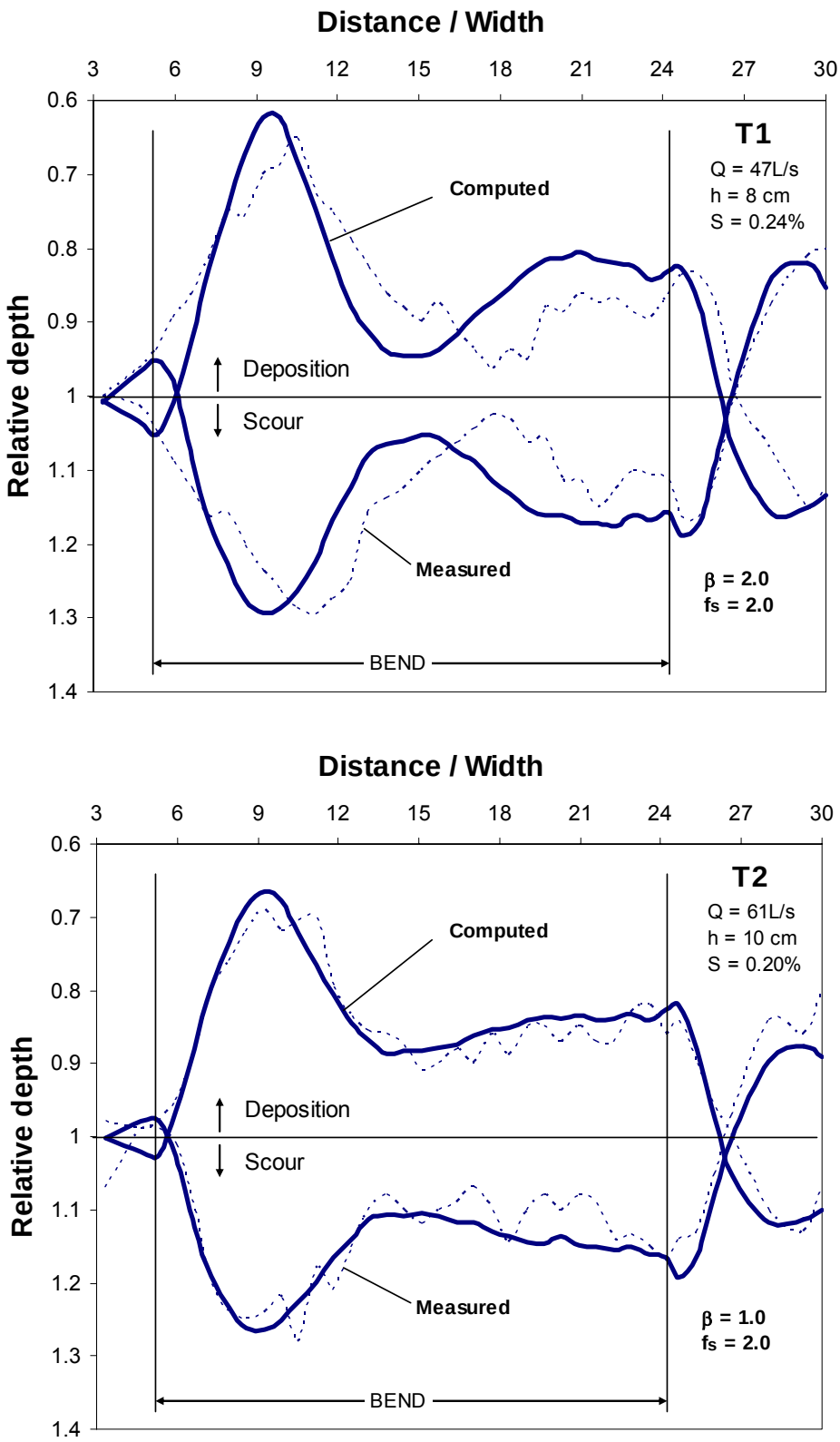

Figure 2. Comparison between the computed and measured longitudinal bed profiles for DHL flume, experiments T1 and T2. Profiles are 0.375 m from right and left banks.

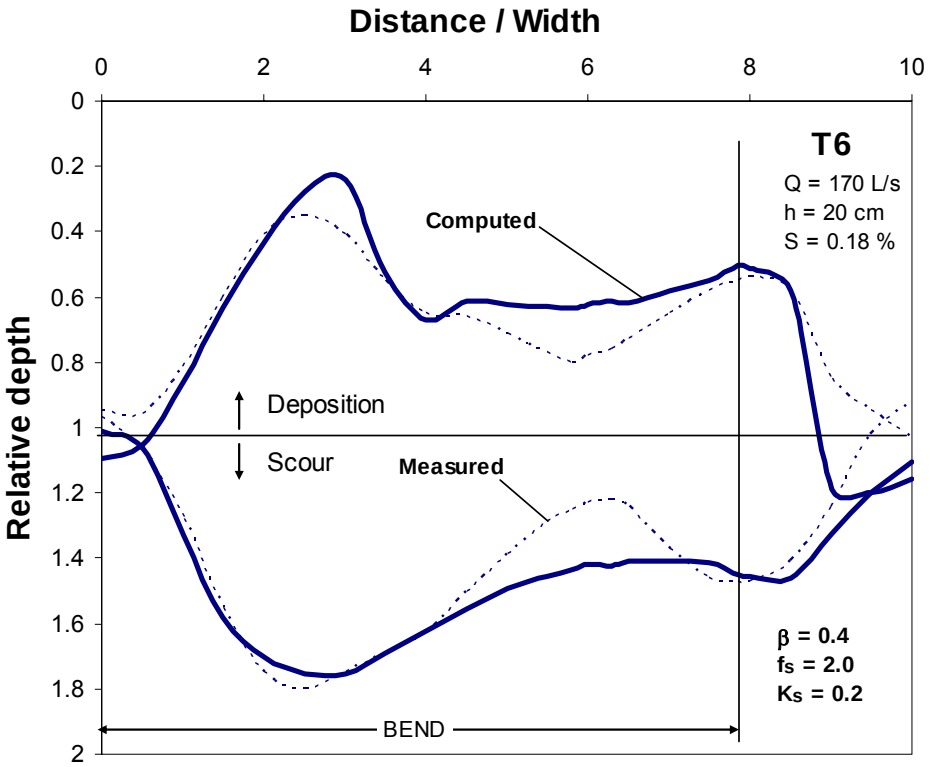

Figure 3. Comparison between the computed and measured longitudinal bed profiles for LFM flume, experiment T6. Profiles are 0.34 m from right and left banks.

Although it is unknown if a migrating bar was observed during the experiment T1; there are experimental observations of bars migrating along bends. Whiting and Dietrich (1993) reported migrating bars in a large amplitude meandering bend with a width to depth ratio of B/h = 17. However, the bars remained static when B/h = 15. Those results seem to agree with our numerical findings, as we observed a migrating bar for experiment T1 (B/h = 19), but not for experiments T2 (B/h = 15) or T6 (B/h = 9). In a recent numerical simulation, Darby et al. (2002) applied Delft Hydraulics' 2D model RIPA to Whiting and Dietrich (1993) experiments, but they were unable to reproduce the migration of bars along the bend, which they admitted was a significant limitation of the model. Encouraged by our initial results, we are planning to make future tests of River2D-MOR to bar migration.

In general, the inclination of the transversal bed slope S_t oscillates along the bend. From an initial flat bed upstream ($S_t = 0$), the transversal slope tends towards and equilibrium value ($S_t \rightarrow S_{te}$) in the bend. However, depending on the flow and sediment conditions, the local value of the transversal slope may overshoot ($S_t > S_{te}$) downstream of the entrance (Struiksma et al. 1985, Parker and Johannesson 1989, Struiksma 1989), causing a large point bar in the inner bank and a deep pool in the outer bank, which can be observed looking at the measured profiles in Figures 2 and 3. Around the center of the bend S_t reaches a minimum value, to increase again around the bend exit. All those features were captured by River2D-MOR, especially for the DHL flume (Fig. 2). For the LFM flume, the minimum value of S_t around the mid-bend was not clearly reproduced (Fig. 3).

River2D-MOR seems to have problems to accurately reproduce the bed oscillations for the strongly curved LFM flume. Similar results were also obtained recently by Kassem and Chaudhry (2002) when simulating experiment T6; although their model underestimated the scour and deposition at the bend exit, which does not happen in our case.

Quantitatively, the magnitude of the maximum scour and deposition seems to be accurately predicted for experiment T2 and T1. For T6, the model slightly over-predicts the height of the point bar. This lower prediction accuracy can be attributed to the high flow curvature of experiment T6.

2D depth average models require the application of secondary flow sub-models, which are normally limited to small flow curvatures. This limitation is because conventional secondary flow sub-models neglect the feedback mechanism between the primary and secondary flows. The secondary flow not only re-circulates mass, but also re-distributes momentum from the primary flow. Momentum is advected from the top fast moving layer of the flow, towards the bottom slow moving layers. This re-distribution of momentum flattens the vertical distribution velocity, which in turn limits the intensity of the secondary flow. i.e., the secondary flow intensity does not grow indefinitely, but becomes self-limited when curvature increases (Blanckaert and Graf 2004).

An alternative way to enhance the capabilities of a 2D depth-average model for flow in bends is the application of the moment-of-momentum (MOM) approach (Ascanio and Kennedy 1982, Jin and Steffler 1993, Ghamry and Steffler 2003, Ghamry and Steffler 2005). Ghamry and Steffler (2005) have demonstrated that solving additional equations for the MOM allows a 2D depth average model to simulate better the velocity redistribution of the primary velocity, but also the tendency of the secondary motion over the vertical profile. We have already developed and tested a 2D morphological model using the MOM hydrodynamic model of Ghamry and Steffler (2005), that will show its capabilities when it is published.

Although River2D-MOR did not provide perfect agreement for some of the experiments, the results provided by the model are probable accurate enough for most practical engineering applications. Moreover, the LFM flume represents an extreme case of high curvature ($h/R_c = 1/21$). In natural rivers, the radius of curvature is usually several orders of magnitude larger than the flow depth (Yalin 1992), leading to very small values of h/R_c, even smaller than those of the DHL flume. Therefore, River2D-MOR should provide good results for applications to real meandering rivers (some initial tests are confirming that).

5. SUMMARY

Combining the results reported in this and the companion paper (Vasquez et al. 2005), the capabilities of the new River2D-MOR model can be summarized as follows:

- The model uses a flexible unstructured mesh that can accommodate almost any planform geometry of natural rivers. The mesh can be easily refined around areas where more detailed is sought, for example in areas with strong gradients.

- The upstream boundary condition can be set as free or with an imposed sediment load. The latter condition allows simulating cases of aggradation or degradation caused by changes in the upstream sediment supply, e.g. below a dam.

- The transcritical flow capabilities of the model make it possible to deal with problems involving supercritical flow and hydraulic jumps, which is rather uncommon for most 2D models. Potential applications of this capability are the simulation of bed changes after dam removal or after landslides in mountain rivers.

- The capability to compute the local radius of curvature of the streamlines from the flow field should allow River2D-MOR to easily model real meandering rivers of varying curvature (simpler models usually assume the meandering river as a series of connected circular segments of constant curvature).

- River2D-MOR can simulate the effects of the secondary flow and the transversal bed slope in the morphology of alluvial bends at a level appropriate enough for most engineering applications of

natural rivers with low curvature. Although at the moment the model is limited to bedload dominated flows and uniform sediment.

- The model is prepared to incorporate in the future any type of sediment transport equation; including complex predictors for multiple sizes of sediment, which would allow the simulation of phenomena such as armouring or bend sorting.

6. REFERENCES

Ascanio, M.F. and Kennedy, J. F. 1982. *Flow in alluvial-river curves*. *Journal of Fluid Mechanics*, 133: 1-16.

Blanckaert, K. and Graf, W.H. 2004. Momentum transport in sharp open channel bends*. Journal of Hydraulic Engineering*, ASCE, 130: 186-198.

Darby, S.E., Alabyan, A.M. and Van de Wiel, M.J. 2002. Numerical simulation of bank erosion and channel migration in meandering rivers. *Water Resources Research*, AGU, 38:2.1-2.21.

Jin, Y.C. and Steffler, P.M. 1993. Predicting flow in curved open channels by depth-averaged method. *Journal of Hydraulic Engineering*, ASCE, 119: 109-124.

Johannesson, H. and Parker, G. 1989. Linear theory of river meanders. *River Meandering*, AGU Water Resources Monograph, Washington, DC, 181-213.

Kassem, A.A. and Chaudhry, M.H. 2002. Numerical modeling of bed evolution in channel bends. *Journal of Hydraulic Engineering*, ASCE, 128: 507-514.

Koch, F.G. and Flokstra, C. 1981. Bed level computations for curved alluvial channels. *XIX Congress of the IARH*, New Delhi, India, 2: 357-388.

Ghamry, H.K. and Steffler, P.M. 2003. Two dimensional vertically averaged and moment equations for rapidly varied flows. *Journal of Hydraulic Research*, IAHR, 40: 579-587.

Ghamry, H.K. and Steffler, P.M. 2005. Two-dimensional depth averaged modeling of flow in curved open channels. *Journal of Hydraulic Research*, IAHR, 43: 44-55.

Parker, G. and Johannesson, H. 1989, Observations on several recent theories of resonance and overdeepening in meandering channels. *River Meandering*, AGU Water Resources Monograph, Washington, DC, 379-415.

Rozovskii, J.L. 1957. *Flow of water in bends of open channel*. Academic of Science of the Ukrainian SSR, Kiev.

Steffler, P.M. and Blackburn, J. 2002. *River2D: Two-dimensional depth-averaged model of river hydrodynamics and fish habitats*. University of Alberta, Edmonton, Canada.

Struiksma, N., Olesen, K. W., Flokstra, C., Vriend, H. J. De 1985. Bed deformation in curved alluvial channels. *Journal of Hydraulic Research*. IAHR, 23: 57-79.

Struiksma, N. 1989, Analysis of a 2-D bed topography model for rivers. *River Meandering,* AGU Water Resources Monograph, Washington, DC, 153-180.

Talmon, A.M., Van Mierlo, M.C., Struiksma, N. 1995. Laboratory measurements of the direction of sediment transport on transverse alluvial-bed slopes. *Journal of Hydraulic Research*. IAHR, 33: 495-517

Vasquez, J.A., Millar, R.G. and Steffler, P.M 2005. River2D Morphology, Part I: Straight Alluvial Channels. *17th Canadian Hydrotechnical Conference*, Edmonton, Canada.

Vriend, H. J. De and Struiksma, N. 1983. Flow and bed deformation in river bends. *Rivers '83*, ASCE, 1:810-828.

Whiting, P.J. and Dietrich, W.E. 1993. Experimental studies of bed topography and flow patterns in large-amplitude meanders: 2. Mechanisms. *Water Resources Research*, AGU, 29:3615-3622.

Yalin, M.S. 1992. *River Mechanics*. Pergamon Press, Oxford, New York.